9-2017

Phylogenetic convergence and multiple shell shape optima for gliding scallops (Bivalvia: Pectinidae)

J. M. Serb
Iowa State University, serb@iastate.edu

E. Sherratt
Iowa State University

A. Alejandrino
Iowa State University

D. C. Adams
Iowa State University, dcadams@iastate.edu

Phylogenetic convergence and multiple shell shape optima for gliding scallops (Bivalvia: Pectinidae)

Abstract

How often, and to what extent, do similar ecologies elicit distantly related taxa to evolve towards the same phenotype? Alike phenotypes can arise when species exploit a common trophic niche and evolutionarily respond in a congruent manner to those selective constraints required for particular function or biomechanical task (Herrel et al., 2008; Vincent et al., 2009; Adams & Nistri, 2010). This is the pattern of convergence, the repeated evolution towards similar phenotypes among multiple lineages that ancestrally lack the trait (Stayton, 2015). As such, convergent evolution is regularly treated as evidence for adaptation (Harvey & Pagel, 1991; Larson & Losos, 1996). Some of the best known examples of convergent evolution are seen in the similarity in body plans of the succulent plants in Euphorbiaceae and Cactaceae (Alvarado-Cárdenas et al., 2013) and Old and New World anteaters (Beck et al., 2006), or the similarity of skull shape between the marsupial Thylacine (Tasmanian wolf) and that of the placental canids (Wroe & Milne, 2007; Goswami et al., 2011).

Disciplines

Biostatistics | Ecology and Evolutionary Biology | Evolution | Population Biology

Comments

This is the peer reviewed version of the following article: Serb, J. M., Sherratt, E., Alejandrino, A. and Adams, D. C. (2017), Phylogenetic convergence and multiple shell shape optima for gliding scallops (Bivalvia: Pectinidae). J. Evol. Biol., 30: 1736–1747, which has been published in final form at doi:10.1111/jeb.13137 .

Phylogenetic convergence and multiple shell shape optima for gliding scallops (Bivalvia : Pectinidae)

J.M. Serb, E. Sherratt, A. Alejandrino, and D.C. Adams

Journal of Evolutionary Biology
2018

Introduction

How often, and to what extent, do similar ecologies elicit distantly related taxa to evolve towards the same phenotype? Alike phenotypes can arise when species exploit a common trophic niche and evolutionarily respond in a congruent manner to those selective constraints required for particular function or biomechanical task (Herrel *et al.*, 2008; Vincent *et al.*, 2009; Adams & Nistri, 2010). This is the pattern of convergence, the repeated evolution towards similar phenotypes among multiple lineages that ancestrally lack the trait (Stayton, 2015). As such, convergent evolution is regularly treated as evidence for adaptation (Harvey & Pagel, 1991; Larson & Losos, 1996). Some of the best known examples of convergent evolution are seen in the similarity in body plans of the succulent plants in Euphorbiaceae and Cactaceae (Alvarado-Cárdenas *et al.*, 2013) and Old and New World anteaters (Beck *et al.*, 2006), or the similarity of skull shape between the marsupial Thylacine (Tasmanian wolf) and that of the placental canids (Wroe & Milne, 2007; Goswami *et al.*, 2011).

However, convergence need not create perfect morphological replicas. Rather, there can be varying degrees of morphological variance among phenotypes even if they experience selective regimes that impose similar or identical functional demands. For example, lineages may converge towards a general area of morphospace, but occupy different regions within it (Herrel *et al*., 2004; Leal *et al*., 2002; Stayton, 2006). Likewise, independent lineages may evolve to a

distinct region in morphospace, but the size of this region may be larger than what the morphospace is for the ancestral phenotypes of those lineages (Collar *et al*., 2014). Furthermore, when multiple levels of biological organization are compared, one may observe convergence in the ability to perform a particular task across a set of taxa, even when such taxa exhibit distinct or even divergent morphologies (reviewed in Wainwright, 2007). In some cases, the disconnect across the functional-morphological boundary can occur when modular morphological components are present, allowing for distinct combinations of morphological forms to create similar functional properties (see e.g., Alfaro *et al*., 2004; Wainwright *et al*., 2005).

For evolutionary biologists, quantifying convergent patterns has long been an analytical challenge, and numerous approaches have been suggested to characterize particular attributes that inform on patterns and processes of convergence (Stayton, 2006, 2008; Muschick *et al.*, 2012; Arbuckle *et al.*, 2014). However, several recently-developed synthetic quantitative measures have been proposed which characterize the overall extent to which two or more lineages display convergent morphological patterns (Stayton, 2015). Importantly, these approaches are process-neutral; describing only patterns of convergence, and leveraging the shared phylogenetic history of the taxa under investigation when making evolutionary inferences of those patterns (see Stayton, 2015). As such, these tools provide a powerful means of evaluating evolutionary convergence, and provide key evidence in determining the extent to which independent lineages converge on a common phenotype or display a suite of closely related solutions to similar ecological challenges.

One the strongest illustrations for how functional demands influence morphology is the many instances of convergent shell form of bivalved molluscs (Bivalvia). It has long been recognized that there is a strong association between shell form and ecological niche in bivalves

(Verrill, 1897; Kauffman, 1969; Stanley, 1970, 1972). Stanley (1970) was the first to described in detail how particular shell traits are found in species belonging to one of seven "life habit" classes (*sensu* Stanley, 1970), which are defined by the animal's life position relative to the substrate, type of locomotion or attachment, and feeding mode (hereafter referred to as "ecomorphs" *sensu* Williams, 1972). Thus, shell form is the evolutionary response to the external requirements for living space, locomotion, defense, and survival of the adult animal. Modifications to shell morphology include changes to the overall outline of each valve (left vs. right), the form along the hinge, the degree of shell inflatedness (convexity vs. concavity), or the extent of ornamentation over each valve. In ecological classes with more specific performance needs, there is a greater opportunity for convergent shell forms (Stanley, 1972; Thomas, 1978; Serb *et al.*, 2011). Thus, performance may be a strong predictor of the degree of shell shape convergence.

Within scallops (Bivalvia: Pectinidae), one striking example of convergent evolution is found in species displaying high-performance swimming, or gliding, behavior (Serb *et al.*, 2011; Mynhardt *et al.*, 2015). This behavior is characterized by the expulsion of water from the mantle cavity while the valves are closed, allowing the animal to propel forward with the ventral-edge leading (Manuel & Dadswell, 1993; Cheng *et al.*, 1996). The biomechanic properities of gliding have been extensively studied, and we have a good understanding of the parameters important to maximize performance (Morton, 1980; Joll, 1989; Hayami, 1991; Millward & Whyte, 1992; Manuel & Dadswell, 1993; Cheng *et al.*, 1996; Ansell *et al.*, 1998; Himmelman *et al.*, 2009; Guderley & Tremblay, 2013; Tremblay *et al.*, 2015). Intriguingly, some measurements of gliding kinematics vary within the ecomorph (Caddy, 1968; Morton, 1980; Joll, 1989; Ansell *et al.*, 1998; Mason *et al.*, 2014), suggesting that there are differences among the functional

components of locomotion (see results below). However, it is unknown whether these differences are the result of variation in shell shape, or other functionally-relevant morphological traits (Guderley & Tremblay, 2013). Collectively, species in the gliding ecomorph have a qualitatively similar shell form that is discoid in shape, lacks prominent external shell surface sculpture, and have a left valve that is slightly more convex than the lower right valve (Stanley, 1970; Gould, 1971). In this instance where there appears to be a tight association between shell shape and performance, the morphology would be predicted to be under strong selection, resulting in a narrow area of occupied morphospace for gliding lineages.

Interestingly, the phylogenetic history of the gliding form across the Pectinidae is uncertain, but a recent phylogenetic analysis revealed that the behavior has evolved independently in at least four lineages: *Adamusium*-*Placopecten*, *Amusium*, *Euvola*, and *Ylistrum* (Alejandrino *et al*., 2011). Previous work (Serb *et al*., 2011) has shown that morphological similarities in shell shape occur between two gliding lineages (*Amusium* and *Ylistrum*; Fig 1b-d), but at the time a more comprehensive phylogenetic framework, as well as the necessary analytical tools (*sensu* Stayton, 2015), were lacking to rigorously test the hypothesis of more widespread morphological convergence in the group. In this study, we test predictions emerging from the hypothesis that shell shape similarity in gliding scallops is the result of evolutionary convergence, using expanded taxon sampling which includes all five genera with gliding species. We adopt an integrative approach combining 3-D geometric morphometric techniques to quantify shell shape variation and phylogenetic comparative methods to infer the history of morphological diversification across species. With this approach we test the following predictions: 1) if gliding has specific biomechanic requirements, then lineages with this life style exhibit morphological convergence in shell shape; 2) if a narrow range of morphologies fulfill

the requirements for gliding, then shell morphologies of gliding species will exhibit less shell shape variation, and taxa will therefore occupy a more restricted region of morphospac, than non-gliding ecomorphs; and 3) if differences in shell shape are related to differences in how gliding is performed biomechanically, then gliding lineages will have evolved multiple anatomical solutions for a common biomechanical challenge. To quantitatively address these hypotheses, we utilize phylogenetic comparative methods for evaluating trends in high-dimensional multivariate data (Adams, 2014a; b), new methods for evaluating morphological disparity in a phylogenetic context, as well as several recently-developed measures that evaluate the degree of evolutionary convergence relative to what is expected based on the phylogeny for the group (Stayton, 2015). Our findings reveal strong evidence for evolutionary convergence in shell shape of gliding species, in which gliding lineages follow similar trajectories to not one, but two regions of morphological space. This pattern suggests that there may be two optima for the gliding phenotype in the Pectinidae.

Materials and Methods

Specimen selection and morphological characterization: A total of 933 specimens from 121 species were used in this study, and were selected to represent a wide range of taxa displaying all six ecomorphs exhibited in the Pectinidae (data from Sherratt *et al.*, 2016) (natural history museums listed in Table S1 and Acknowledgments. For each specimen, shell morphology was quantified using geometric morphometric methods (Bookstein, 1991; Mitteroecker & Gunz, 2009; Adams *et al.*, 2013). These methods utilize the locations of landmark coordinates as the basis of shell shape quantification. The method is identical to Sherratt *et al*. (2016), and uses a total of 202 landmarks and semilandmarks to characterize shell shape (Fig. 1). Briefly, we first obtained high-resolution scans of the left valves of each individual using a NextEngine 3D

surface scanner. From these scans we then digitized the locations of five homologous anatomical locations following Serb *et al*. (2011): 1: ventroposterior auricle, 2: dorsoposterior auricle, 3: umbo, 4: dorsoanterior auricle, 5: ventroanterior auricle (Fig. 1). Next, twelve semilandmarks were placed equidistantly between these fixed points to capture the shape of the auricles, and 35 equidistant points were placed along the ventral edge of the valve between the anterior and posterior auricles. Finally, we used an automated procedure to fit 150 semi-landmarks to the shell surface using a template; these are allowed to slide in 3D over the surface (Gunz *et al.*, 2005; Serb *et al.*, 2011; Sherratt *et al.*, 2016).

To obtain a set of shape variables for each specimen, we aligned the 933 landmark configurations using a generalized Procrustes analysis (GPA: Rohlf & Slice, 1990). Procrustes superimposition removes differences in specimen position, orientation, and scale, and aligns all specimens to a common coordinate system. During this analysis, the semilandmarks were permitted to slide along their tangent directions using the Procrustes distance criterion. The aligned specimens were then projected orthogonally to tangent space to obtain a set of shape variables (Procrustes tangent coordinates: Rohlf, 1990) for use in all subsequent analyses. Specimen digitizing and GPA were performed in R 3.3.2 (R Core Team, 2017) using the package *geomorph* v.3.0.3 (Adams & Otárola-Castillo, 2013; Adams *et al.*, 2016).

Statistical Analyses: Overall patterns of variation in shell shape were visualized in morphospace using a principal components analysis (PCA). However, because species are not independent of one another, all subsequent statistical analyses evaluating our evolutionary hypotheses were conducted on species means and using a phylogenetic comparative framework. To evaluate morphological trends in a phylogenetic context, we performed several phylogenetic comparative analyses, using a multi-gene molecular phylogeny containing 143 species of

Pectinidae (Fig. S1; Table S2) (Alejandrino *et al*,. 2011; Sherratt *et al*., 2016). Briefly, we constructed a robust, time-calibrated phylogeny using sequence data from two mitochondrial genes (12S, 16S ribosomal RNAs) and two nuclear genes (histone H3, 28S ribosomal RNA) which were obtained from museum specimens using procedures in Puslednik and Serb (2008) and Alejandrino *et al*. (2011). Sequence data were aligned using CLUSTAL W (Thompson *et al.*, 1994) in Geneious Pro v.5.6.4 (http://www.geneious.com) (Kearse *et al.*, 2012) with a gap-opening penalty of 10.00 and a gap-extending penalty of 0.20. GBlocks Server (Talavera & Castresana, 2007) was used to remove ambiguous alignment in 16S rRNA. For Bayesian inference, we used a relaxed clock model as implemented in BEAST v.1.8.0 (Drummond & Rambaut, 2007) with a speciation model that followed incomplete sampling under a birth-death prior and rate variation across branches uncorrelated and exponentially distributed. Three independent simulations of Markov Chain Monte Carlo for 20 million generations were run, sampling every 100 generations, and 20,000 trees were discarded as burn-in using Tracer v.1.6 l (Rambaut *et al.*, 2014). The remaining trees were combined in LogCombiner; the best tree was selected using TreeAnnotator. We used 30 fossils to constrain the age of nodes through assigning node priors, details of which are in Sherratt *et al.* (Table 2 in 2016).

Combining the morphological and phylogenetic data, the mean shell shape was estimated for each species and the morphological dataset was matched to the phylogeny. As there were 93 species shared between the two datasets, and the phylogeny and the morphological data matrix were pruned to contained the unique set of 93 taxa (Fig. 2, as in Sherratt *et al*. 2016). Phylogenetic patterns of shell shape evolution were examined using several approaches. First, to evaluate phylogenetic trends in the shape data we first conducted an analysis of phylogenetic signal, using the multivariate version of the *kappa* statistic (K_{mult}: (Adams, 2014a). Next, we

performed a phylogenetic analysis of variance (ANOVA) to evaluate whether shell shape differed among ecomorphs while accounting for phylogenetic non-independence. This approach is based on a generalization of phylogenetic generalized least squares (PGLS), and is appropriate for evaluating trends in high-dimensional multivariate data (described in Adams, 2014; Adams & Collyer, 2015). We visualized patterns of shell shape evolution using a phylomorphospace approach (*sensu* Sidlauskas, 2008), where the extant taxa and the phylogeny were projected into morphospace, and evolutionary changes in shape were visualized along the first two axes of this space using PCA.

Finally, we performed several quantitative analyses to evaluate the degree of morphological convergence in a phylogenetic context, including two recently-developed convergence measures (Stayton, 2015). The first convergence measure, C_1 (Stayton, 2015), characterizes the degree of morphological difference between extant taxa relative to the maximal morphological distance between any of their ancestors. This measure represents the proportion of morphological divergence that has been reduced in the extant taxa, with a maximal value (1.0) indicating the extant species are morphologically identical (Stayton, 2015). The second convergence measure, C_5 (Stayton, 2015), describes the frequency of convergence into a particular region of morphospace, and is estimated by determining the number of extant lineages of the putatively convergent taxa that cross the boundary of a convex hull formed by the focal taxa (Stayton, 2015). Both measures were statistically evaluated using phylogenetic simulation, where multivariate datasets are simulated along the phylogeny using Brownian motion, and the observed test measures are compared to a distribution of possible values obtained from these simulations to assess their significance (Stayton, 2015).

Additionally, we evaluated whether the degree of morphological disparity (Stayton, 2006; see also Zelditch *et al.*, 2012) among species in the gliding ecomorph was less than expected by chance while accounting for phylogenetic relatedness using two novel approaches. For the first approach, we estimated the observed morphological disparity among species within each ecomorph, and ranked the degree of disparity in the gliding ecomorph relative to the disparity observed within all other ecomorphs. Then, we generated 1000 simulated datasets under a Brownian motion model of evolution, using the time-dated molecular phylogeny above and an input covariance matrix based on the covariance matrix of the observed shape data. From each dataset, we then estimated measures of morphological disparity for each ecomorph, and compared the observed patterns of disparity to what was expected under a Brownian motion model of evolution (for a related procedure see: Garland Jr. *et al.*, 1993; Sherratt *et al.*, 2016).

Our second approach accounted for the phylogeny directly in the disparity calculations. Here, we performed a transformation of the data using the phylogenetic transformation matrix (Garland, Jr., & Ives, 2000; see also Adams, 2014b), and obtained estimates of disparity for each ecomorph in the phylogenetically-transformed space following standard computations. The significance of phylogenetic morphological disparity for the gliding ecomorph was then evaluated statistically using permutation tests, where morphological values were permuted across the tips of the phylogeny to disassociate the morphological data from the ecomorph groups (see Adams, 2014a). Note that our procedure for phylogenetic morphological disparity differ from that of Brusatte *et al*. (2017), in that our approach directly accounts for species' non-independence due to the phylogeny when estimating patterns of morphological diversity in extant taxa. By contrast, Brusatte *et al.* (2017) use estimated ancestral states to inform disparity measures among fossils at particular time periods in the paleontological history of a group, but

did not incorporate the phylogeny in extant analyses directly. All analyses were performed in R 3.3.2 (R Core Team, 2017) using the package *geiger* 2.0.6 (Pennel *et al.*, 2014), the package *geomorph* v.3.0.3 (Adams & Otárola-Castillo, 2013; Adams *et al.*, 2016), the package *convevol* v.1.0 (Stayton, 2014), and routines written by one of the authors (DCA).

Biomechanical data and analysis: In addition to morphological data we obtained several measurements of functional performance in swimming for four species of gliding scallops (*A. pleuronectes, Ad. colbecki, P. magellanicus,* and *Y. balloti*). Performance measures were taken from the primary literature, and were based on swimming trials of animals in the laboratory (Morton, 1980) or under natural conditions (Joll, 1989; Ansell *et al.*, 1998; Mason *et al.*, 2014). Data collected by SCUBA divers and high-definition video recordings include: distance traveled, the number of adductions during the swimming bout, swimming time, and swimming velocity. Because data from some publications were presented only as means and standard deviations, we performed t-tests comparing pairs of taxa for each performance measure.

Results

Visual inspection of morphospace using PCA revealed distinct clusters that broadly corresponded to the ecomorph groups (Fig. 3). Specifically, the free-living and byssal attaching ecomorphs occupied most of the morphospace and overlapped greatly in PC1 vs PC2, but showed some separation along PC3. The recesser ecomorph formed an elongate cluster extending away from the main cloud of free/byssal species. The specimens of ***Pedum spondyloideum***, the only nestling species, were all very different from one another, and lay at the edge of the free-living/byssal attaching ecomorph cloud, as did species of the cementing ecomorph (see full list in Supplementary Materials, Table S1).

The gliding ecomorph occupies the extreme positive end of PC2 where valves have smaller auricles compared to other ecomorphs. Interestingly, these gliding individuals occupied two distinct regions of morphospace. This implies that two sub-clusters of similar, yet subtly distinct shell shapes were exhibited by species that utilize this behavior. The shape difference between the two gliding morphotypes was described by the degree of valve flatness (Z-axis), where flatter valves were at the positive end of PC1 (Fig. 3, lateral views). Further, gliding species appeared to display less variation in shell shape when compared to the other ecomorphs, as the patterns of distribution in morphospace of the two clusters were each more restricted compared to other ecomorphs.

Across scallops, shell shape displayed significant phylogenetic sigal (K_{mult} = 0.2778; P <0.001). Using phylogenetic ANOVA, we found significant differences in shell shape across ecomorphs (D-PGLS, $F_{5,87}$ = 5.505, P < 0.001, R^2 = 0.240, Z = 8.60), implying that the functional groups were morphologically distinct in spite of shared evolutionary history. When viewed in phylomorphospace (Fig. 4), the shell shape differences were evident, with the gliding species occupying a unique region of morphospace when compared to taxa from the other functional groups. Lending support to this visual observation, both measures of convergence for the gliding taxa revealed strong evolutionary signals for morphological similarity in gliding species. Specifically, the average measure C_1 between pairs of gliding taxa was 0.45, indicating that the distance between extant gliding species is on average 45% less of morphospace when compared to the maximum spread of their ancestors. Using Brownian motion simuations, this value was highly significant (P > 0.001). Likewise, the number of convergent events in gliding species (C_5 = 5) was significantly greater than would be expected from a Brownian motion model of evolution (P = 0.016). Additionally, gliding species displayed the lowest levels of

within-ecomorph disparity (Table 1), and this pattern differed significantly from what was expected under a Brownian motion model of evolution ($P = 0.031$). Further, when morphological disparity was evaluated in a phylogenetic context, there was less variation within the gliding ecomorph than expected by a random association of morphology and ecotype ($MD_{glide} = 3.28 \times 10^{-5}$; $P = 0.004$: Table 1). Taken together, these analyses provided significant empirical support for the hypothesis that species in the gliding ecomorph displayed phylogenetic evolutionary convergence.

Interestingly, as was observed in the PCA of all individuals, phylogenetic patterns in shell shape viewed in phylomorphospace (Fig. 4) revealed two clear clusters of gliding species. One of these clusters (the 'A' morphotype) was comprised of four species derived from three distinct phylogenetic lineages [*Ylistrum ballotti* (Bernardi, 1861) & *Y. japonicum* (Gmelin, 1791); *Amusium pleuronectes* (Linnaeus, 1758); *Euvola papyraceum* Gabb, 1873] (species d, c, b, and a, respectively, in Fig. 2) (Pectininae; see Serb, 2016). The 'B' gliding morphotype was comprised of species from two Tribes [Adamussiini: *Adamussium colbecki* (Smith, 1902) & Palliolini: *Placopecten magellanicus* (Gmelin, 1791)] (Serb, 2016) (species e and f: Fig. 2). Thus, patterns of phenotypic evolution of shell shape appeared to display two distinct gliding morphologies. Interestingly, we observed significant differences in biomechanical performance measures between species in these two morphotypes, with the A morphotype attaining greater distances, displaying a higher number of adductions, longer swim times, and faster velocities then the B morphotype (Table 3). Taken together, these results imply that there are two two gliding morphs in scallops, and each has accomplished their gliding behavior differently from a biomechanical perspective.

Discussion

Morphological convergence provides a series of independent tests of the phenoptypic response to a particular selective regime. In phenotypes where performance level is determined by the morphology of the organism, strong selective forces may act on specific components of that form. In the case of gliding scallop species, this hypothesis is supported. Specifically, we found significant similarity in shell shape across these species in a manner suggestive of evolutionary convergence. Further, explicit tests of evolutionary convergence revealed that the observed similarities were unlikely if traits evolved under multivariate Brownian motion, lending additional support to the convergence hypothesis. Together our results are consistent with the prediction that locomotory performance elicits selection on shell morphology, resulting in evolutionary convergence in shell shape in those species which have independently evolved gliding behavior. Interestingly, while gliding taxa do occupy a distinct region in morphospace from scallop species exhibiting other behaviors, the evolution of the gliding form in Pectinidae is not a simple example of convergence. Rather, there is still some additional structure within the gliding morphotype suggestive of both overall convergence in shell shape, as well as a degree morphological divergence (a relatively flat valve with small auricles, and the degree of valve flatness, respectively). This latter finding is evidenced by the fact that two clusters of gliding taxa are evident in phylomorphospace (Fig. 4; see also Fig. 3), and that species in these two clusters display significant differences in biomechanical performance (Table 3). Thus, while there is a clear gliding morphotype displayed across all gliding lineages, sub-forms within this group are also apparent.

From these observations, we can draw three conclusions. First, morphological convergence in shell shape does occur for the five gliding lineages, and lineages occur in a

distinct, but broad, region of morphospace, separate from other life habit forms. Second, while all gliding species occupy the same general region of morphospace, among the gliders, two morphotypes can be distinguished. This implies that two subtle, yet distinct shell shapes are exhibited by species that must solve the same performance challenges related to the gliding behavior. Third, gliding has more restrictive shell form requirements than other life habits. Gliding species display less variation in shell shape when compared to the other life habits. Indeed, the two gliding morphotypes had roughly 30% of the variation observed in the other life habit groups, indicating a significant reduction in shell shape variation among gliding individuals. Overall, both the individual-based patterns (Fig. 3) and the phylomorphospace pattern (Fig. 4) suggest that there may be two optima for the gliding phenotype in the Pectinidae.

Interestingly, the limited performance data on gliding in scallops is consistent with our two optima hypothesis implied by the morphological data. Several parameters of functional performance in swimming have been evaluated in these taxa, and slight differences in these biomechanical parameters exist between the gliding species including: the maximum distance traveled of a single swim, the number of adductions per swimming effort, and horizontal swimming speed (Caddy, 1968; Morton, 1980; Joll, 1989; Ansell *et al.*, 1998) (Table 2). Further, the differences in performance observed between taxa also correspond to the two gliding morphotypes found in this study. When placed in the context of our morphological findings, it is clear that the two gliding morphotype differ in how they locomote. Specifically, the data examined here suggest that members of morphotype A (*A. pleuronectes, E. papyraceum, Y. balloti,* and *Y. japonicum)* can swim faster and for longer distances than members of morphotype B (*P. magellanicus, Ad. colbecki*) (Tables 2-3). We hypothesize this may be a direct result of a more effective gliding phase due to shells having a more discoid and hydrodynamic form

through the reduction of the auricles (and other conclusions from our results). This hypothesis has support from previous work by Hayami (1991), who found *Y. japonicum* (morphotype A) shells have the lower value of drag coefficient and higher lift-drag ratio when compared to *P. magellanicus* (morphotype B), which is likely to be because morphotype A is flatter than B. Future biomechanical studies directly linking gliding performance with three-dimensional shell shape would be essential in testing these observations and this hypothesis.

A central conclusion of our study is that the shell shape of gliding scallops exhibits a strong pattern of convergence. Quantifying convergence is important not only for identifying major evolutionary trends, but to discover, and subsequently measure, the more subtle degrees of morphological convergence. This variation can then be placed into the relevant biological context and direct future research efforts. However, the challenge has been to apply a pattern-based, rather than process-based, approach. The recent development of quantative, pattern-based evolutionary convergence tests finally provides us with a useful set of tools to evaluate convergence within a phylogenetic context (Stayton, 2015). This approach has been used successfully to quantify convergent evolution across ecological guilds in a wide variety of taxa including pythons and boas (Esquerré *et al.*, 2016), planktivorous surgeonfishes (Friedman *et al.*, 2016), social swallows (Johnson *et al.*, 2016) and squirrels (Zelditch *et al.*, 2017). Thus, the application of quantitative measures should illuminate convergence patterns in understudied taxa and provide key evidence in determining the extent to which independent lineages converge on a common phenotype or display a suite of closely related solutions to similar ecological challenges.

Acknowledgements

We are very grateful for the assistance and loans provided by the staff of museums and research institutions, especially J. McLean and L. Groves [LACM]; G. Paulay and J. Slapcinsky [FLMNH]; E. Shea, N. Aziz and L. Skibinski [DMNH]; S. Morrison and C. Whisson [WAM]; E. Strong, T. Nickens, P. Greenhall and T. Walter [NMNH]; E. Lazo-Wasem [YMP]; G.T. Watters [OSUM]; P. Bouchet and P. Maestrati [MNHM]; A. Baldinger [MCZ]; M. Siddall and S. Lodhi [AMNH]; R. Bieler and J. Gerber [FMNH]; R. Kawamoto [BPBM]; E. Kools [CAS]; and A. Bogan and J. Smith [NCSM]. Organization and collection of molecular and morphological data were aided by the team of undergraduate researchers: K. Boyer, D. Brady, K. Cain, G. Camacho, N. Dimenstein, C. Figueroa, A. Flander, A. Frakes, C. Grula, M. Hansel, M. Harmon, S. Hofmann, J. Kissner, N. Laurito, N. Lindsey, S. Luchtel, C. Michael, V. Molian, A. Oake, J. Rivera, H. Sanders, M. Steffen and C. Wasendorf. We thank C.P. Klingenberg and two anonymous reviewers for helpful comments on an earlier version of this manuscript. Authors declare no conflict of interest.

References

Adams, D. 2014a. A generalized K statistic for estimating phylogenetic signal from shape and other high-dimensional multivariate data. *Syst. Biol.* **63**: 685–697.

Adams, D. 2014b. A method for assessing phylogenetic least squares models for shape and other high-dimensional multivariate data. *Evolution (N. Y).* **68**: 2675–2688.

Adams, D. & Otárola-Castillo, E. 2013. geomorph: an R package for the collection and analysis of geometric morphmetric shape data. *Methods Ecol. Evol.* **4**: 393–399.

Adams, D., Rohlf, F.J. & Slice, D.E. 2013. A field comes of age: Geometric morphometrics in the 21st century. *Hystrix* **24**: 7–14.

Adams, D.C. & Collyer, M.L. 2015. Permutation tests for phylogenetic comparative analyses of high-dimensional shape data: What you shuffle matters. *Evolution (N. Y).* **69**: 823–829.

Adams, D.C., Collyer, M.L., Kaliontzopoulou, A. & Sherratt, E. 2016. geomorph 3.0.3: software for geometric morphometric analyses.

Adams, D.C. & Nistri, A. 2010. Ontogenetic convergence and evolution of foot morphology in European cave salamanders (Family: Plethodontidae). *BMC Evol. Biol.* **10**: 1–10.

Alejandrino, A., Puslednik, L. & Serb, J.M. 2011. Convergent and parallel evolution in life habit of the scallops (Bivalvia: Pectinidae). *BMC Evol. Biol.* **11**: 164.

Alfaro, M.E., Bolnick, D.I. & Wainwright, P.C. 2004. Evolutionary dynamics of complex biomechanical systems: an example using the four-bar mechanism. *Evolution* **58**: 495–503.

Alvarado-Cárdenas, L.O., Martínez-Meyer, E., Feria, T.P., Eguiarte, L.E., Hernández, H.M., Midgley, G., *et al.* 2013. To converge or not to converge in environmental space: Testing for similar environments between analogous succulent plants of North America and Africa. *Ann. Bot.* **111**: 1125–1138.

Ansell, A.D., Cattaneo-Vietti, R. & Chiantore, M. 1998. Swimming in the Antartic scallop Adamussium colbecki analysis of in situ video recordings. *Antarct. Sci.* **10**: 369–375.

Arbuckle, K., Bennett, C. & Speed, M. 2014. A simple measure of the strength of convergent evolution. *Methods Ecol. Evol.* **5**: 685–693.

Beck, R.M.D., Bininda-Emonds, O.R.P., Cardillo, M., Liu, F.-G.R. & Purvis, A. 2006. A higher-level MRP supertree of placental mammals. *BMC Evol. Biol.* **6**: 93.

Bernardi, C. 1861. *Journal de Conchyliologie.* P.-H. Fischer., [Paris].

Bookstein, F.L. 1991. *Morphometric tools for landmark data: geometry and biology*. Cambridge University Press, Cambridge.

Brusatte, S.L., Montanair, H.-Y. & Norell, M. 2017. Phylogenetic corrections for morphological disparity analysis: new methodology and case studies. *Paleobiology* **37**: 1–22.

Caddy, J.F. 1968. Underwater observations on scallop (Placopecten magellanicus) behavior and drag efficiency. *J. Fish. Res. Board Canada* **25**: 2123–2141.

Cheng, J., Davison, I.G., Demont, M.E. & Chang, J.-Y. 1996. Dynamics and energetics of scallop locomotion. *J. Exp. Biol.* **199**: 1931–1946.

Collar, D.C., Reece, J.S., Alfaro, M.E., Wainwright, P.C. & Mehta, R.S. 2014. Imperfect morphological convergence: variable changes in cranial structures underlie transitions to durophagy in moray eels. *Am. Nat.* **183**: E168-84.

Drummond, A.J. & Rambaut, A. 2007. BEAST: Bayesian evolutionary analysis by somping

trees. *BMC Evol. Biol.* **7**: 214.

Esquerré, D., Scott Keogh, J. & Harmon, L. 2016. Parallel selective pressures drive convergent diversification of phenotypes in pythons and boas. *Ecol. Lett.* **19**: 800–809.

Friedman, S.T., Price, S.A., Hoey, A.S. & Wainwright, P.C. 2016. Ecomorphological convergence in planktivorous surgeonfishes. *J. Evol. Biol.* **29**: 965–978.

Garland, Jr., T. & Ives, A.R. 2000. Using the past to predict the present: Confidence intervals for regression equations in phylogenetic comparative methods. *Am. Nat.* **155**: 346–364.

Garland Jr., T., Dickerman, A.W., Janis, C.M. & Jones, J.A. 1993. Phylogenetic analysis of covariance by computer simulation. *Syst. Biol.* **42**: 265–292.

Gmelin, J.F. 1791. *Caroli a Linné, systema naturae. Tom. I. Pars VI.* Lipsiae [Leipzig] :

Goswami, A., Milne, N. & Wroe, S. 2011. Biting through constraints: cranial morphology, disparity and convergence across living and fossil carnivorous mammals. *Proc. Biol. Sci.* **278**: 1831–1839.

Gould, S.J. 1971. Muscular mechanics and the ontogeny of swimming in scallops. *Palaeontology* **14**: 61–94.

Guderley, H.E. & Tremblay, I. 2013. Escape responses by jet propulsion in scallops. *Can. J. Zool.* **91**: 420–430.

Gunz, P., Mitteroecker, P. & Bookstein, F.L. 2005. Semilandmarks in three dimensions. In: *Modern morphometrics in physical anthropology* (D. E. Slice, ed), pp. 73–98. Klewer Academic/Plenum Publishers, New York.

Harvey, P.H. & Pagel, M.D. 1991. *The comparative method in evolutionary biology*. Oxford University Press, Oxford.

Hayami, I. 1991. Living and fossil scallop shells as airfoils: an experimental study. *Paleobiology* **17**: 1–18.

Herrel, A., Vanhooydonck, B. & Van Damme, R. 2004. Omnivory in lacertid lizards: Adaptive evolution or constraint? *J. Evol. Biol.* **17**: 974–984.

Herrel, A., Vincent, S.E., Alfaro, M.E., Wassenbergh, S. Van, Vanhooydonck, B. & Irschick, D.J. 2008. Morphological convergence as a consequence of extreme functional demands: examples from the feeding system of natricine snakes. *J. Evol. Biol.* **21**: 1438–1448.

Himmelman, J.H., Guderley, H.E. & Duncan, P.F. 2009. Responses of the saucer scallop Amusium balloti to potential predators. *J. Exp. Mar. Bio. Ecol.* **378**: 58–61.

Johnson, A.E., Mitchell, J.S. & Brown, M.B. 2016. Convergent evolution in social swallows (Aves: Hirundinidae). *Ecol. Evol.* 550–560.

Joll, L.M. 1989. Swimming behavior of the saucer scallop Amusium balloti (Mollusca, Pectinidae). *Mar. Biol.* **102**: 299–305.

Kauffman, E.G. 1969. Form, function, and evolution. In: *Treatis on Invertebrate Paleontology, Part N, Mollusca 6, Bivalvia* (R. C. Moore, ed), pp. N130–N205. Geological Society of American and University of Kansas, Lawrence, KS.

Kearse, M., Moir, R., Wilson, A., Stones-Havas, S., Cheung, M., Sturrock, S., *et al.* 2012. Geneious Basic: An integrated and extendable desktop software platform for the organization and analysis of sequence data. *Bioinformatics* **28**: 1647–1649.

Larson, A. & Losos, J.B. 1996. Phylogenetic systematics of adaptation. In: *Adaptation* (M. R. Rose & G. V Lauder, eds), pp. 187–220. Academic Press, San Diego.

Leal, M., Knox, A.K. & Losos, J.B. 2002. Lack of convergence in aquatic Anolis lizards. *Evolution* **56**: 785–791.

Linnaeus, C. 1758. *Systema Naturae per Regna tria naturae, secundum classes, ordines, genera, species, cum characteribus, differentiis, synonymis, locis [...] Tomus I, Editio Decima, Reformata*.

Manuel, J.L. & Dadswell, M.J. 1993. Swimming of juvenile sea scallops, Placopecten magellanicus (Gmelin) - a minimum size for effective swimming. *J. Exp. Mar. Bio. Ecol.* **174**: 137–175.

Mason, G.E., Sameoto, J.A. & Metaxas, A. 2014. In situ swimming characteristics of the sea scallop, Placopecten magellanicus, on German Bank, Gulf of Maine. *J. Mar. Biol. Assoc. United Kingdom* **94**: 1019–1026.

Millward, A. & Whyte, M.A. 1992. The hydrodynamic characteristics of six scallops in the superfamily Pectinacea, Class Bivalvia. *J. Zool.* **227**: 547–566.

Mitteroecker, P. & Gunz, P. 2009. Advances in Geometric Morphometrics. *Evol. Biol.* **36**: 235–247.

Morton, B. 1980. Swimming in Amusium pleuronectes (Bivalvia: Pectinidae). *J. Zool.* **190**: 375–404.

Muschick, M., Indermauer, A. & Salzburger, W. 2012. Convergent evolution within an adaptive radiation of cichlid fish. *Curr. Biol.* **22**: 1–7.

Mynhardt, G., Alejandrino, A., Puslednik, L., Corrales, J. & Serb, J. 2015. Shell shape convergence masks biological diversity in gliding scallops: description of Ylistrum n.gen. (Pectinidae) from the Indo-Pacific Ocean. *J. Molluscan Stud.*

Pennel, M., Eastman, J., Slater, G., Brown, J., Uyeda, J., Fitzjohn, R., *et al.* 2014. geiger v2.0: an expanded suite of methods for fitting macroevolutionary models to phylogenetic trees. *Bioinformatics* **30**: 2216–2218.

Puslednik, L. & Serb, J.M. 2008. Molecular phylogenetics of the Pectinidae (Mollusca: Bivalvia) and the effect of outgroup selection and increased taxon sampling on tree topology. *Mol. Phylogenet. Evol.* **48**: 1178–1188.

R Core Team. 2017. R: a language and environment for statistical computing. RFoundation for Statistical Computing, Vienna.

Rambaut, A., Suchard, M., Xie, D. & Drummond, A. 2014. Tracer v1.6, available from http://beast.bio.ed.ac.uk/Tracer.

Rohlf, F.J. 1990. Morphometrics. *Annu. Rev. Ecol. Syst.* **21**: 299–316.

Rohlf, F.J. & Slice, D.E. 1990. Extensions of the Procrustes method for the optimal superimposition of landmarks. *Syst. Zool.* **39**: 40–59.

Serb, J. 2016. Reconciling morphological and molecular approaches to develop a phylogeny for the Pectinidae (Mollusca: Bivalvia). In: *Scallops: Biology, Ecology and Aquaculture* (G. J. Parsons & S. E. Shumway, eds), pp. 1–29. Elseiver.

Serb, J.M., Alejandrino, A., Otárola-Castillo, E. & Adams, D.C. 2011. Shell shape quantification using geometric morphometrics reveals morphological convergence of distantly related scallop species (Pectinidae). *Zool. J. Linn. Soc.* **163**: 571–584.

Sherratt, E., Alejandrino, A., Kraemer, A., Adams, D. & Serb, J. 2016. Trends in the sand: directional evolution in the shell shape of recessing scallops (Bivalvia: Pectinidae). *Evolution (N. Y).* **70**: 2061–2073.

Sidlauskas, B. 2008. Continuous and arrested morphological diversification in sister clades of characiform fishes: A phylomorphospace approach. *Evolution (N. Y).* **62**: 3135–3156.

Smith, E. 1902. Report on the collections of natural history made in the Antarctic region during the voyage of the “Southern Cross.” In: *Mollusca* (I. Franklin, ed), pp. 201–213.

Stanley, S.M. 1972. Functional morphology and evolution of bysally attached bivalve mollusks. *J. Paleontol.* **46**: 165–212.

Stanley, S.M. 1970. Relation of shell form to life habits of the Bivalvia (Mollusca). *Geol. Soc. Am. Mem.* **125**: 1–296.

Stayton, C.T. 2014. convevol: Quantifies and assesses the significance of convergent evolution. R package version 1.0. Available at http://cran.r-project.org/web/packages/convevol/index.html.

Stayton, C.T. 2008. Is convergence surprising? An examination of the frequency of convergence in simulated data sets. *J. Theor. Biol.* **252**: 1–14.

Stayton, C.T. 2006. Testing hypotheses of convergence with multivariate data: morphological and functional convergence among herbivorous lizards. *Evolution (N. Y).* **60**: 824–841.

Stayton, C.T. 2015. The definition, recognition, and interpretation of convergent evolution, and two new measures for quantifying and assessing the significance of convergence. *Evolution (N. Y).* **69**: 2140–2153.

Talavera, G. & Castresana, J. 2007. Improvement of phylogenies after removing divergent and ambiguously aligned blocks from protein sequence alignments. *Syst. Biol.* **56**: 564–77.

Thomas, R.D.K. 1978. Shell form and the ecological range of living and extinct Arcoida. *Paleobiology* **4**: 181–194.

Thompson, J.D., Higgins, D.G. & Gibson, T.J. 1994. CLUSTAL W: improving the sensitivity of progressive multiple sequence alignment through sequence weighting, position-specific gap penalties and weight matrix choice. *Nucleic Acids Res.* **22**: 4673–4680.

Tremblay, I., Samson-Dô, M. & Guderley, H.E. 2015. When behavior and mechanics meet: scallop swimming capacities and their hinge ligament. *J. Shellfish Res.* **34**: 203–212.

Verrill, A.E. 1897. A study of the family Pectinidae, with a revison of genera and subgenera. *Trans. Connect. Acad. Arts Sci.* **10**: 41–95.

Vincent, S.E., Brandley, M.C., Herrel, A. & Alfaro, M.E. 2009. Convergence in trophic morphology and feeding performance among piscivorous natricine snakes. *J. Evol. Biol.* **22**: 1203–1211.

Wainwright, P.C. 2007. Functional Versus Morphological Diversity in Macroevolution. *Annu. Rev. Ecol. Evol. Syst.* **38**: 381–401.

Wainwright, P.C., Alfaro, M.E., Bolnick, D.I. & Hulsey, C.D. 2005. Many-to-one mapping of form to function: A general principle in organismal design? *Integr. Comp. Biol.* **45**: 256–262.

Williams EE. 1972. The origin of faunas. Evolution of lizard congeners in a complex island fauna: A trial analysis. *Evol. Biol.* **6**: 47–89.

Wroe, S. & Milne, N. 2007. Convergence and remarkably consistent constraint in the evolution of carnivore skull shape. *Evolution (N. Y).* **61**: 1251–1260.

Zelditch, M.L., Swiderski, D.L. & Sheets, H.D. 2012. *Geometric Morphometrics for Biologists: A Primer*, 2nd ed. Academic Press.

Zelditch, M.L., Ye, J., Mitchell, J.S. & Swiderski, D.L. 2017. Rare ecomorphological convergence on a complex adaptive landscape: body size and diet mediate evolution of jaw shape in squirrels (Sciuridae). *Evolution (N. Y).*, doi: 10.1111/evo.13168.

Tables

Table 1 Levels of morphological disparity (MD) among species within each ecomorph. The first row represents MD obtained using standard approaches while the second row contains measures obtained while accounting for phylogenetic non-independence among taxa. MD for the nestling ecomorph is not shown, as there was only one species represented in this study.

Ecomorph	Byssal attaching	Cementing	Free-living	Gliding	Recessing
MD: Standard	2.144×10^{-3}	2.079×10^{-3}	3.593×10^{-3}	1.937×10^{-3}	2.036×10^{-3}
MD: Phylogenetic	6.515×10^{-5}	3.949×10^{-5}	1.055×10^{-4}	3.286×10^{-5}	1.186×10^{-4}

Table 2 Some aspects of swimming performance during the horizontal phase in gliding scallops from the A and B morphotypes (indicated in parentheses).

	A. pleuronectes (A)*	*Y. balloti* (A) †	*P. magellanicus* (B)‡	*Ad. colbecki* (B) ¶
Distance traveled (m)	1-10 N/A	1.0-23.1 mean = 8.01 ± 4.57 (n = 200)	0.26-3.26 mean = 1.44 ± 0.599 (n = 126)	0.11-2.03 mean = 0.276 ± 0.14 (n = 9)
Number of adductions	10-50 mean = 22.968 ± 9.816 (n = 29)	N/A	8-21§ mean = 13.38 ± 3.49 (n = 32)	1-18 mean = 2.44 ± 1.24 (n = 9)
Swimming time (s)	5-18 mean = 9.72 ± 3.1327 (n = 32)	N/A	1.2-7.4 mean = 3.1 ± 1.2 (n = 126)	0.86-10.16 mean = 1.72 ± 0.78 (n = 9)
Swimming velocity (m/s)	0.23-0.73 mean = 0.39 ± 0.107 (n = 37)	0.2-1.6 mean = 0.86 ± 0.288 (n = 25)	0.42-1.03 mean = 0.474 ± 0.166 (n = 200)	0.19-0.43 mean = 0.157 ± 0.04 (n = 7)

* Morton, 1980
† Joll, 1989
‡ Mason *et al.* 2014
§ Caddy, 1968
¶Ansell, 1998

Table 3 Results from pairwise t-tests (T) comparing performance measures between members of the A morphotype and the B morphotype. All comparisons were statistically significant at the experiment-wise Bonferroni value ($P < 0.005$) unless indicated.

	Distance traveled		Number of adductions		Swimming time		Swimming velocity	
	T	*P*	T	*P*	T	*P*	T	*P*
Y_balloti (A) vs. *P_magellanicus* (B)	39.54	2.46×10^{-126}	N/A		N/A		3.47	3.08×10^{-4}
Y_balloti (A) vs. *Ad_colbecki* (B)	39.46	1.41×10^{-98}	N/A		N/A		5.35	4.27×10^{-6}
A_pleuronectes (A) vs. *P_magellanicus* (B)	N/A		16.07	1.27×10^{-39}	20.19	1.09×10^{-45}	0.47	0.316 NS
A_pleuronectes (A) vs. *Ad_colbecki* (B)	N/A		29.20	3.06×10^{-27}	18.60	2.61×10^{-21}	1.23	0.112 NS

Figure legends

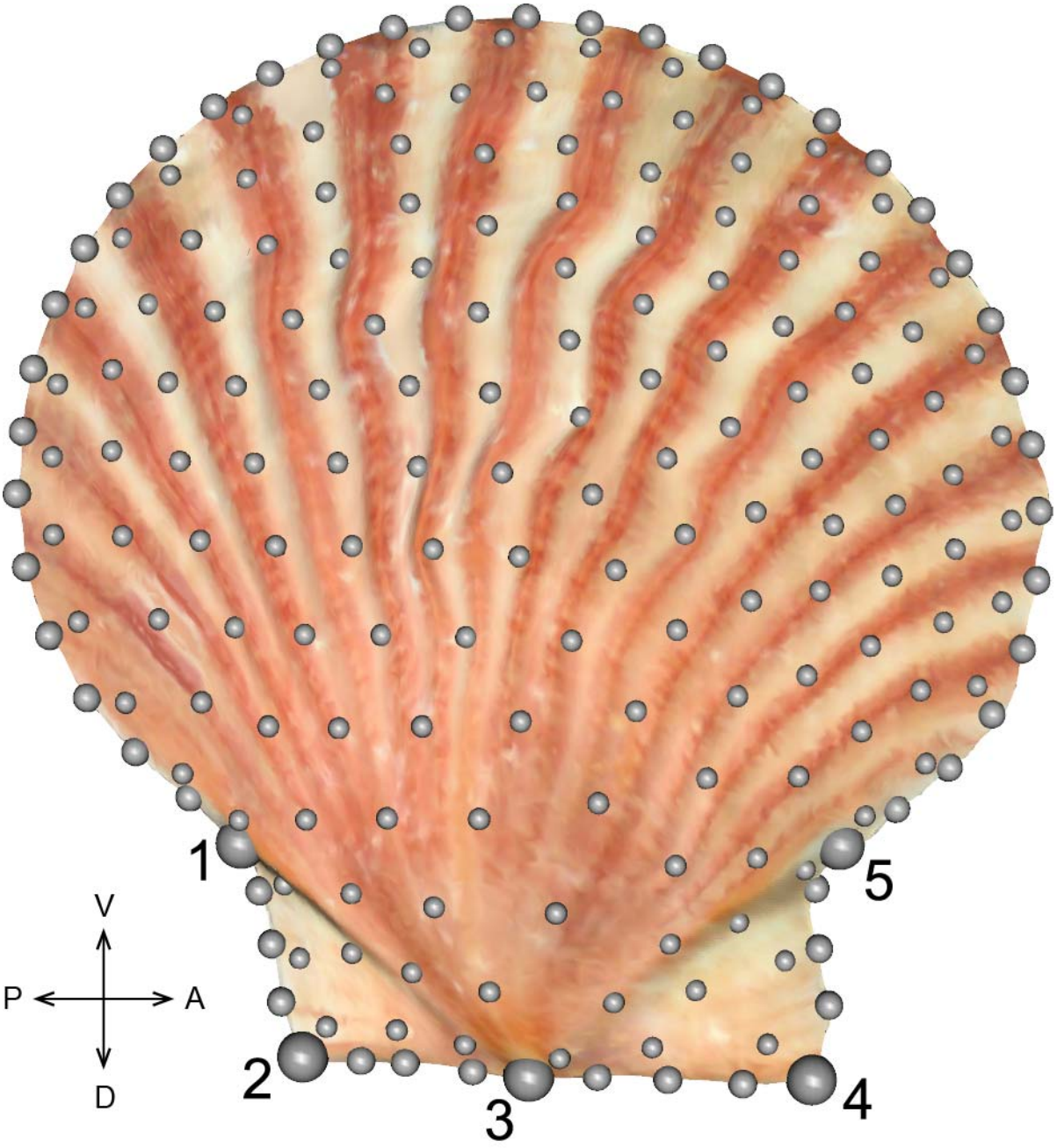

Figure 1 Three-dimensional surface scan of the left valve of a scallop with the position of landmarks and semilandmarks indicated as silver spheres. Five landmarks are numbered and represented by large spheres: Landmark 1 ventroposterior auricle; Landmark 2 dorsoposterior

auricle; Landmark 3 umbo; Landmark 4 dorsoanterior auricle; Landmark 5 ventroanterior auricle. Semilandmarks are shown as small spheres. Redrawn from Sherratt *et al*. (2016).

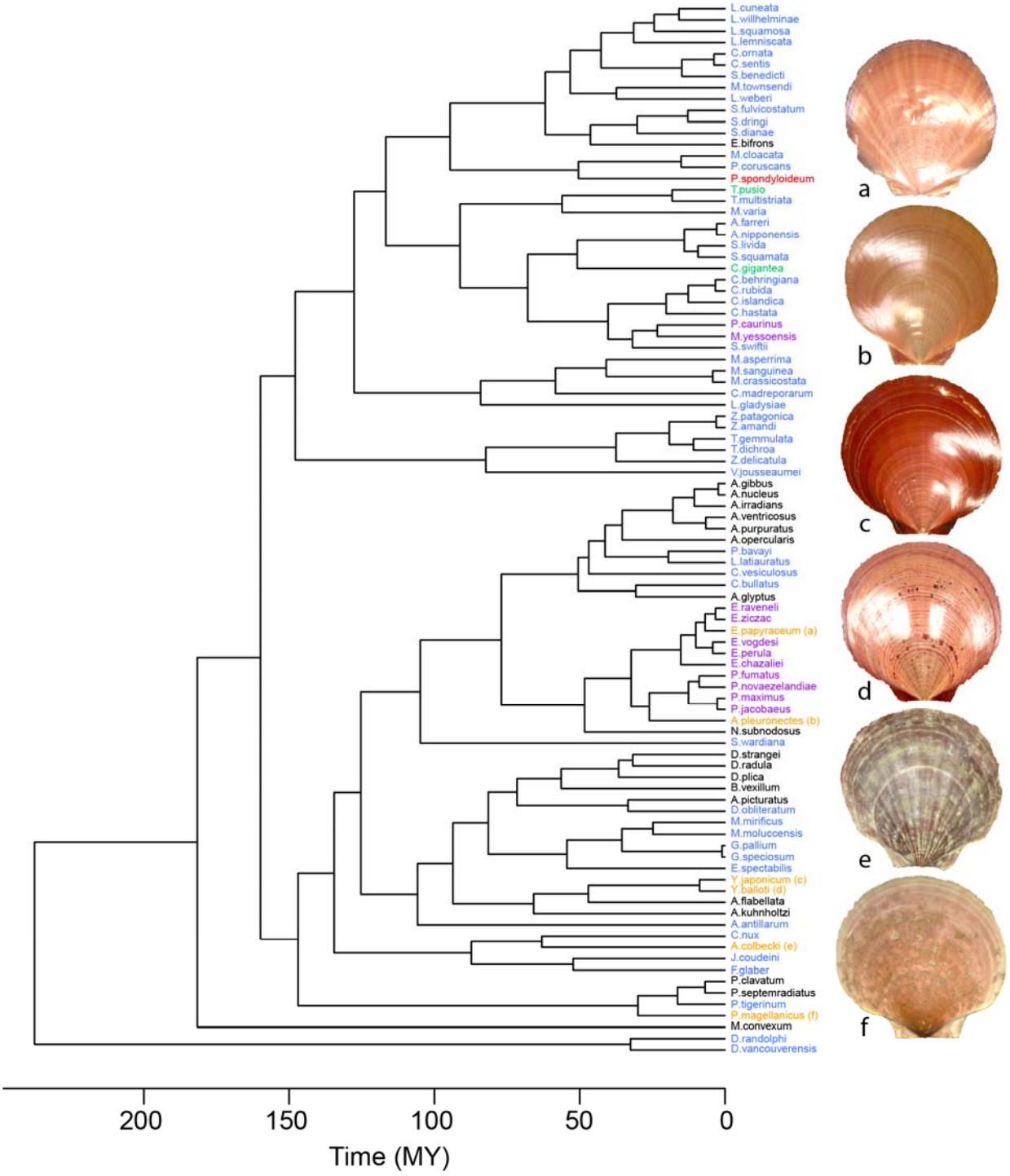

Figure 2 Pruned chronogram of 93 scallop species for which morphological data is available.

Species labels are colored by life habit (green = cementing, red = nestling, blue = byssal attaching, purple = recessing, black = free-living, orange = gliding). Left valves of the six gliding species are shown on the right (marked by letters a-f). Genera and species as in Table S2. Time calibration based upon 30 node groups. Redrawn from Sherratt *et al*. (2016).

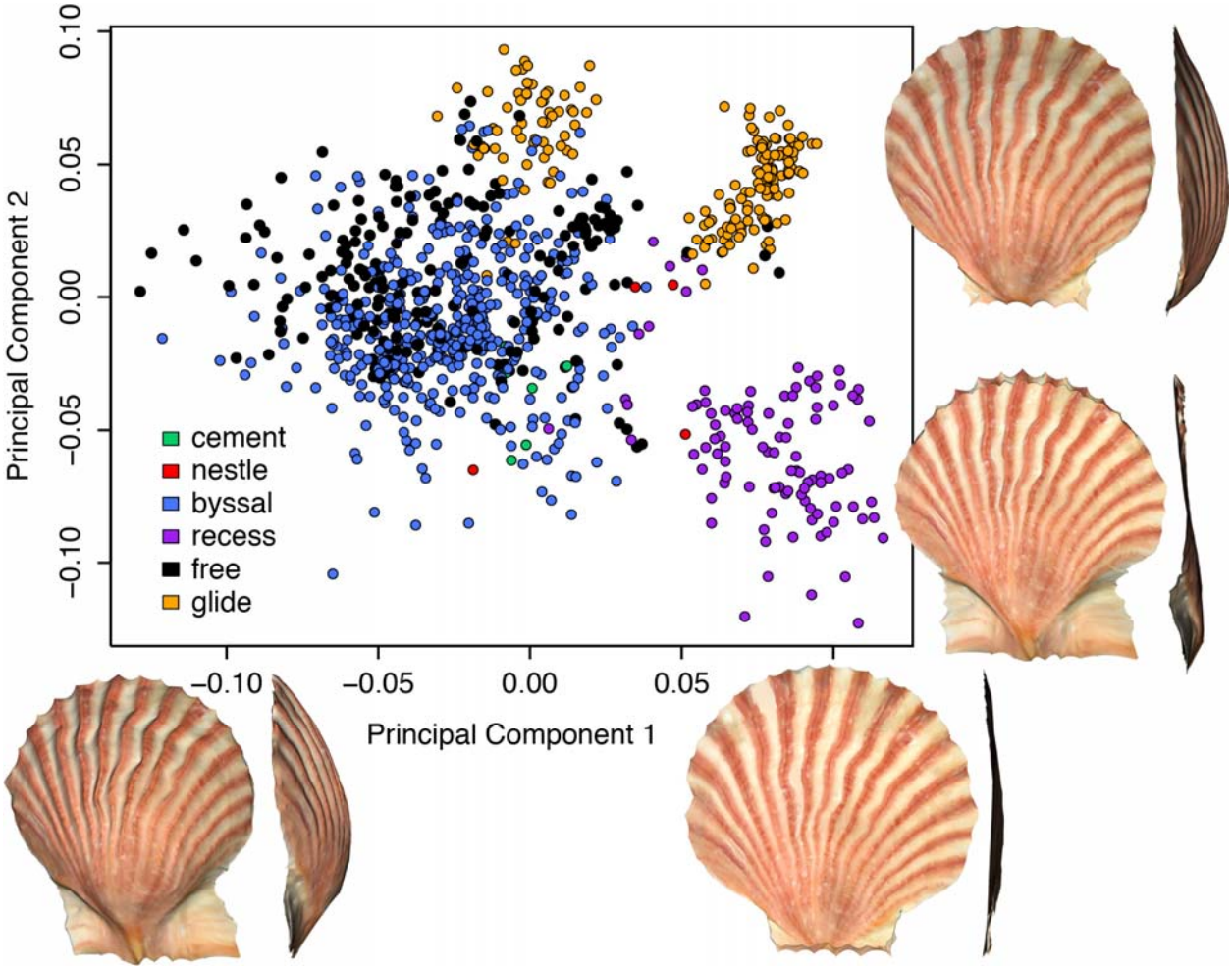

Figure 3 Principal components plot of shell shape based on 933 specimens. The first two axes explain 66.7% of the total shape variation (PC1 = 42%; PC2 = 24.6%). Specimens are colored by the life habit group to which they belong (legend inset, ordered by increasing mobility). Shape deformations relating to the positive and negative extremes of each axis are shown as surfaces warped using thin-plate spline, depicted in dorsal (left) and lateral (right) views.

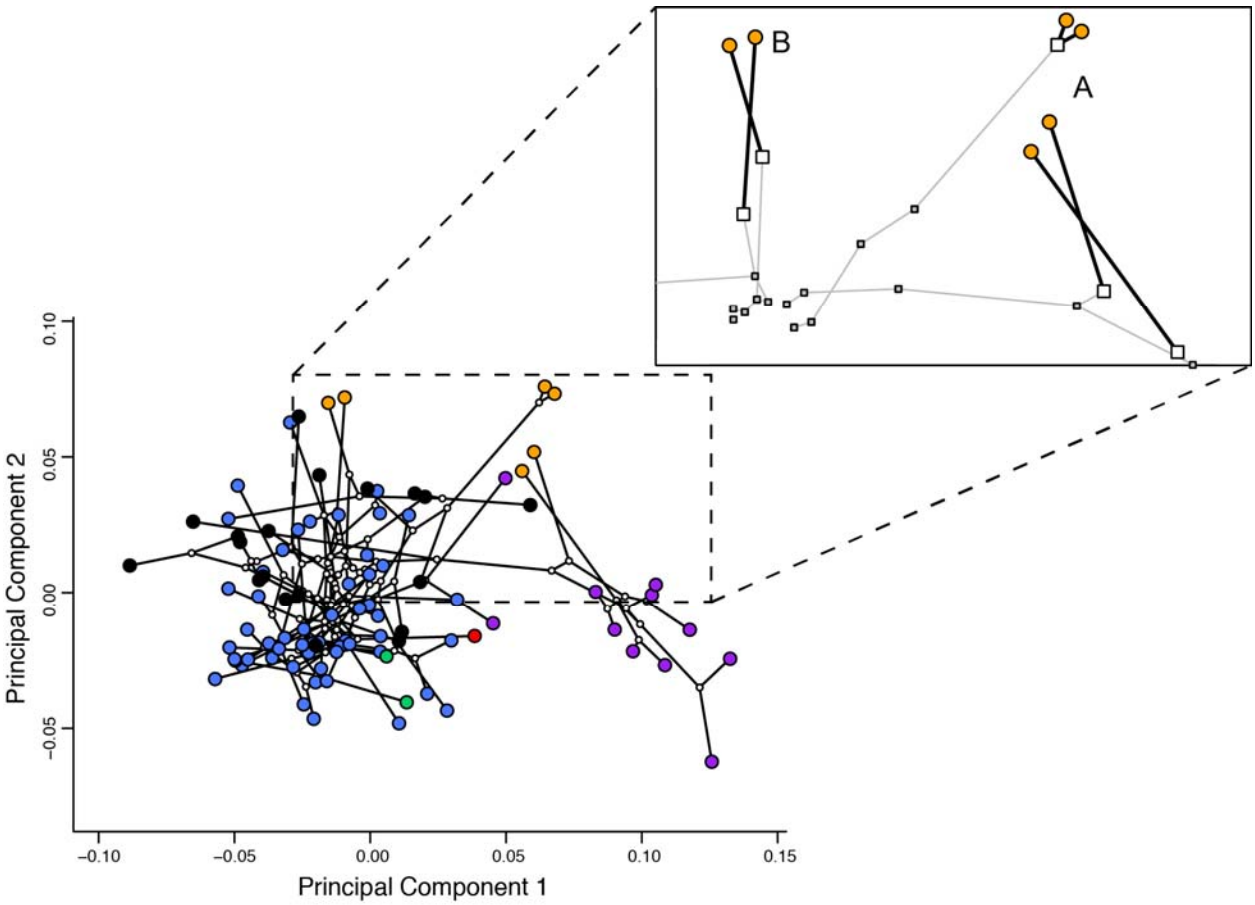

Figure 4 Phylomorphospace plot visualizing the first two axes of morphospace of scallops, with the phylogeny superimposed for 93 species. Colored dots represent extant species and white dots represent hypothesized ancestors inferred from ancestral state reconstruction. The inset shows an enlargement of the region in morphospace containing gliding species with orange dots, displaying the two gliding morphotypes (A and B). Only those phylogenetic branches containing gliding species and their ancestors (squares) are shown.

Supporting information

Additional Supporting Information may be found online in the supporting information tab for this article:

Fig. S1 Chronogram of 143 scallop species.

Fig. S2 Axes 2 and 3 of a principal components plot of shell shape based on 933 specimens, plotted as PC3 *vs* 2 to be compared side-by-side with Figure 3. Together, PCs 1-3 explain 78.8% of the variation (PC2 = 24.6%, PC3 = 12.2%; subsequent axes each contribute less than 5% of the total shape variation). Specimens are colored by the life habit group to which they belong (legend inset, ordered by increasing mobility). Shape deformations relating to the positive and negative extremes of PC3 are shown as surfaces warped using thin-plate spline, depicted in dorsal (left) and lateral (right) views.

Table S1 Scallop behavioral life habit categories for morphological specimens.

Table S2 Genbank accession numbers for 143 specimens included in the molecular phylogeny.

Data deposited at Dryad (need to update): doi:10.5061/dryad.43548.